ABSTRACT

BROWN, MICHELLE R. Viscous Deformation and Electrical Conductivity of MWNT Epoxy Composites. (Under the direction of Jagannadham Kasichainula.)

Viscous deformation behavior and electrical conductivity characteristics of epoxy composites with multiwall nanotube (MWNTs) dispersions were studied. MWNTs were used as an alternative to other filler materials for potential use in high strength and high electrical conductivity applications.

Different mass fractions of MWNT's were dispersed in epoxy matrix using ultrasonication. The MWNT-epoxy composites were oven cured at controlled temperature for up to 10 hours. The composite samples were characterized for dispersion of MWNTs in the epoxy by optical microscopy, transmission electron microscopy (TEM) and Raman spectroscopy. Measurements of electrical conductivity and dynamic mechanical analysis (DMA) were performed as a function of temperature.

The results showed that the MWNT's in the epoxy composites were uniformly distributed with presence of small regions of agglomeration. MWNT-epoxy composites showed four orders of magnitude improvement in electrical conductivity with increase in mass fraction of MWNTs from 1.1×10^{-4} up to 6.6×10^{-3}. The temperature dependence of the electrical conductivity was found to follow both the variable range hoping (VRH) and fluctuation induced tunneling (FIT) models with low activation energy. However, linear dependence of conductivity on the width of the resin barrier separating the MWNTs closely followed the predictions of the FIT model.

DMA measurements showed an increase in the activation energy for viscous deformation with increase in mass fraction of MWNTs. However, the glass transition

temperature (Tg) did not show a systematic increase with increase in the mass fraction of MWNTs. The variation in the dispersion of the MWNTs in the epoxy matrix is thought to be responsible for the absence of a systematic variation of Tg.

The present results indicate that using sonication to disperse MWNT's in an epoxy matrix is a simple process to produce high electrical conductivity epoxy composites.

Viscous Deformation and Electrical Conductivity of MWNT Epoxy Composites

by
Michelle R. Brown

A thesis submitted to the Graduate Faculty of
North Carolina State University
in partial fulfillment of the
requirements for the degree of
Master of Science

Materials Science and Engineering

Raleigh, North Carolina

2012

APPROVED BY:

_____	_____
Dr. Korukonda Murty	Dr. Ronald Scattergood

_____
Dr. Jagannadham Kasichainula Committee Chair

DEDICATION

This thesis is dedicated to my family who supported me in my pursuit of a Masters degree. In addition, I would like to thank my co-workers at BGF Industries, Inc. who also supported and encouraged me.

BIOGRAPHY

Michelle R. Brown was born in Greenville, S.C. on September 11, 1957 and remained there graduating from Greenville Senior High School. In the fall of 1975 she began her college career at Charleston Southern University. In the spring of 1979 she received a Bachelor of Science degree in Chemistry from Charleston Southern University. Upon graduation, Michelle worked for Nutricia as Manager of the Chemistry Laboratory. She left Nutricia and worked for Digital Equipment Corporation as a Senior Research Scientist in the R&D facility. She moved to Greensboro N.C. in 1993 and worked for BGF Industries as Senior Quality & Technical Engineer. She is still employed at BGF Industries, Inc. In the fall of 2008 she began continuing her education at NCSU pursuing a Master of Science degree in Materials Science and Engineering.

ACKNOWLEDGMENTS

I would first like to thank my advisor, Dr. Jag Kasichainula, for all of his guidance and support, during the research. I also want to thank Dr. Korukonda Murty and Dr. Ron Scattergood for being committee members, as well as for their guidance. I thank Dr. Roberto Garcia and Dr. Dale Batchelor for assistance with characterization techniques. I would also like to thank BGF Industries, Inc. for the time to pursue a degree in Materials Science. I also wish to thank Mr. Jacen Busick for serving as my proctor. Finally, I would like to thank my family and friends for their support throughout my graduate studies.

TABLE OF CONTENTS

LIST OF FIGURES

LIST OF TABLES

1. Introduction

1.1 Carbon Nanotube

The use of carbon nanotubes in composites is fueled by their exceptional mechanical and electrical properties. Carbon nanotubes (CNT's) were discovered in 1991 by Iijima [(1)] and are part of a class of molecules composed entirely of carbon. They have a structure of linked hexagonal or pentagonal rings of carbon in tube form. The properties of CNT's arise from the sp^2 hybridized carbon bond. Graphene is similar to this structure and is a one atom thick planar sheet of sp^2 bonded carbon atoms in a honeycomb lattice. CNT's form as a graphene layer with many edge atoms that have dangling bonds. These bonds correspond to a high energy state. The total energy of a graphene layer can be reduced by eliminating the dangling bonds. The formation of a closed structure, such as a CNT, is promoted by this reduction in energy even if the strain energy is increased. Even though CNT's are closely related to graphene the curvature of the tube and quantum confinement along the circumference gives rise to properties that are different from that of graphene [(2)].

CNT's are categorized as single wall (SWNT's) or multi-wall (MWNT's). The cylindrical tubes may have one or both ends capped with a fullerene type hemisphere. Fullerenes are molecules composed entirely of carbon in the form of a sphere. SWNT's are individual tubes that have a single wall consisting of 1 atom thick carbon lattice. MWNT's are nested SWNT's having concentric walls.

CNT structure is compared to wrapping a layer of graphene into a seamless tube configuration.

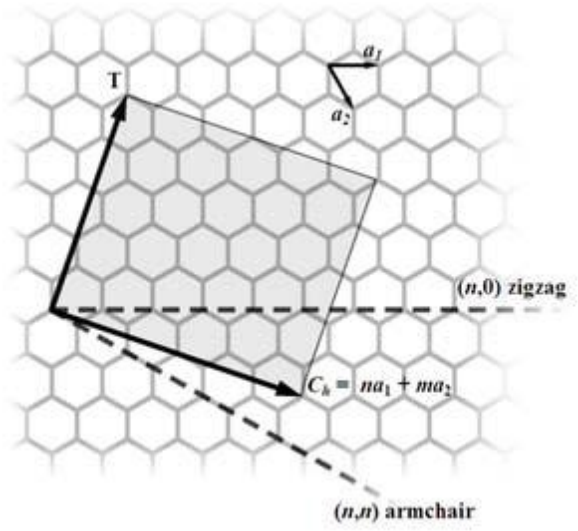

Figure 1.The (*n*,*m*) nanotube naming scheme can be thought of as a vector (**C**h) in an infinite graphene sheet that describes how to "roll up" the graphene sheet to make the nanotube. **T** denotes the tube axis, and **a**1 and **a**2 are the unit vectors of graphene in real space [3]

The resulting nanotubes are considered armchair, if n = m and zigzag if m=0. The n and m designations are indices of the unit vector along the lattice structure of graphene [3] as shown in figure 1. Rolling the lattice at different angles creates a twist or spiral in the nanotube molecular structure. This twist is called chirality[3].

There are two models used to describe MWNTs. The Russian Doll model has sheets of graphene as a nested coaxial array of SWNTs of different radii. In the Parchment model a single sheet of graphene is rolled around on itself. This structure is similar to a scroll or a rolled parchment. The Russian Doll model is more commonly observed in literature. In both models the separation of the tubes is approximately equal to 0.34nm (the interlayer distance of graphene) [5].

1.2 Epoxy Composites

Epoxy is one of the most commonly used polymer systems in a variety of structural and electrical applications. It is an excellent electrical insulator. Today it is used in the manufacture of circuit boards serving as the dielectric between layers. Epoxies are also used to protect electrical components from moisture, dust and contaminants.

Epoxy is a thermosetting polymer formed from a reaction of epichlorhydrin and bisphenol-A. A catalyst containing amine groups (ex: triethylenetetramine) is added where the amine group reacts with the epoxide group to form a covalent bond. The resulting polymer is highly cross-linked, rigid and has high strength.

The present work was performed to add different mass fractions of MWNTs into an epoxy matrix and determine mechanical behavior, glass transition temperature and electrical conductivity. If an effective conductive network can be formed with MWNT's, at a lower mass fraction, this would provide a valuable alternative to other filler materials such as carbon black or carbon fiber. The mechanisms of improvement in electrical conductivity and mechanical strength are investigated.

1.3 Methods of Synthesis of Carbon Nanotubes

Various methods have been developed for synthesis of CNT's. New methods to improve initial purity (carbon content) and reduce secondary or post processing continue to be investigated. Many applications desire SWNTs for their purity and application. MWNT's are produced utilizing the same methods in many cases as production of SWNT's.

Arc Discharge

Iijima observed CNTs in the carbon soot of graphite electrodes in an arc discharge reactor using a current of 100 amps[(1)]. In the arc discharge method of CNT synthesis an electric current is applied across two graphite electrodes in an inert atmosphere, as illustrated in figure 2a. One electrode evaporates as cations which are then deposited at the other electrode. The soot that is formed contained CNT's[(4)]. If a metal such as Co or Mo is used in one of the electrodes, the soot changed composition and more SWNTs than MWNTs were produced. The products of the arc discharge must be further purified due to the complex mixture of unwanted carbon forms and other metal species created in the discharge.

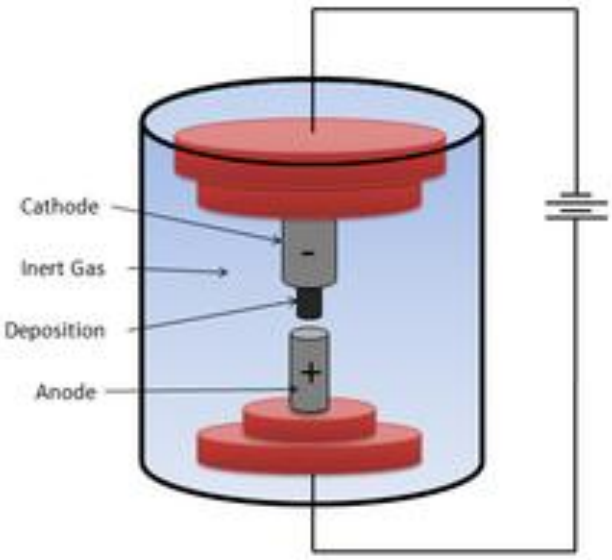

Figure 2(a): Depiction of arc discharge technique for synthesis of carbon nanotubes

Laser Ablation

A pulsed high power laser is used to vaporize carbon from a graphite target in a high temperature environment (approximately 1200^{o}C)[4], as shown in figure 2b. The first laser pulse vaporizes the target and the second pulse breaks up the larger particles ablated by the first laser pulse. Inert gas is fed into the reactor to carry the vaporized carbon to the cooled collector where it condenses. This technique is found to produce both SWNT's and MWNT's. The use of a carbon target containing Co and Ni provides conditions for growth of SWNT's at a high purity level [6].

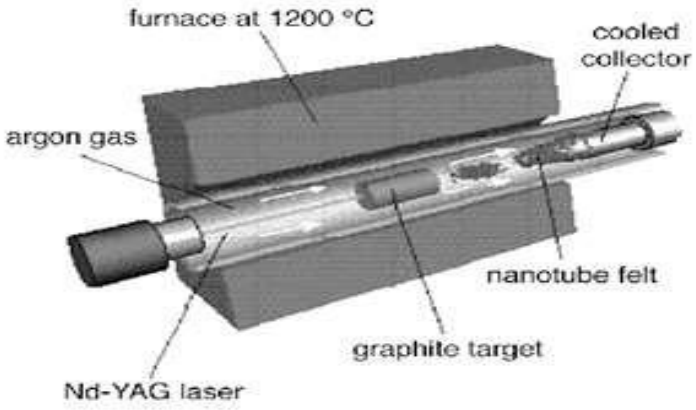

Figure 2(b): Laser ablation method for carbon nanotube synthesis

Chemical Vapor Deposition

Chemical vapor deposition (CVD) is a process that has been used extensively to produce various carbon forms for many years [7]. CVD of hydrocarbons (acetylene, methane, etc) over a substrate with a layer of metal catalyst particles is used to produce large amounts of

CNT's, as illustrated in figure 2c. Cobalt and iron catalysts supported by a silica or aluminosilicate substrate are commonly used. A carbon source such as acetylene, methane, ethanol or ethylene has been shown to be effective for production of CNT's. Catalysts with a single metal or mixture of metals (iron, cobalt, nickel, molybdenum) induce the growth of the CNTs directly on the substrate. Growth of the CNTs directly on the substrate reduces or eliminates much of the post production purification and collection processes [8-10].

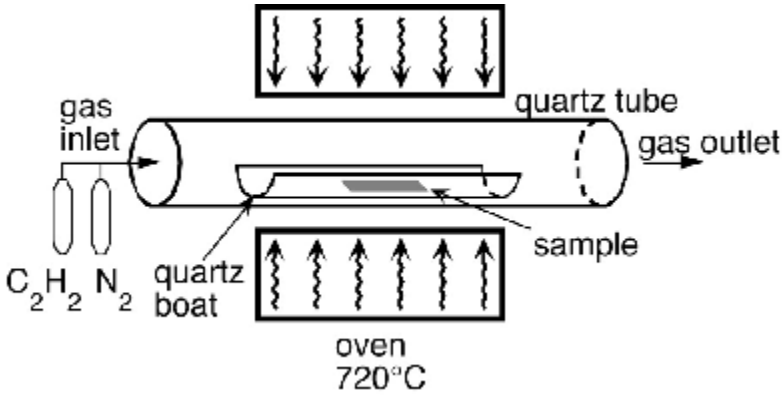

Figure 2(c): Schematic of typical chemical vapor deposition process.

1.4 Electrical Transport Properties

Recent studies on transport properties have been performed with SWNTs & MWNTs using percolation behavior [11]. Percolation behavior is used to describe the electrical conductivity of a disordered system such as a composite.

The electrical conductivity of CNT's varies from semi-conducting to metallic behavior depending on the diameter and chirality of CNT's [4]. The typical MWNT is a concentric

shell having diameter restrictions on the individual tube diameters . MWNT's with a larger diameter (5+nm), as compared to SWNT's (1-2nm), are metallic due to the zero band gap. Theoretical calculations of the conductive ability of metallic CNT's indicate their capability to carry a current density 1000 times greater than that of copper [12]. CNTs have been shown experimentally to exhibit very low electrical resistance [4]. The high electrical conductivity and high mobility of the charge carrier are the result of low probability of scattering from defects in the structure.

Electrical resistance is observed when an electron collides with a defect in the crystal structure or impurity. The aspect ratio (length to diameter) of CNT's is large (~500) so that the electrons have fewer possibilities to scatter. Thus, spatial confinement of electrons gives CNTs their low resistance [4].

Researchers have reported a current carrying capacity of 10^9 amp/cm^2 for SWNT's [13]. As previously noted CNT's may be semiconducting or metallic based on their chirality (either armchair or zigzag). The aspect ratio and size of the CNT aggregates are found to influence the percolation behavior of nanotube composites.

The electrical conductivity in resins [14], films [11], with [15] and without additional fillers (such as carbon black or carbon fibers) [16] has been evaluated to identify the critical concentration for the percolation threshold and analyze the electrical transport mechanisms.

1.5 Mechanical Properties

The mechanical properties of CNT's are strongly dependent on their structure and the method of synthesis since some synthesis methods yield a higher level of defects in the nanotube [17]. The Young's modulus of MWNT's decreases as the disorder within the walls increases [17]. Arc grown MWNT's have fewer defects and the modulus is comparable to that

of SWNTs. Young's modulus of arc grown MWNTs have a reported average value of E = 810 ± 410 GPa [18]. The large polarizability (the response of the electronic structure of CNTs to electric field) of CNT's suggests that the physical interactions, primarily van der Waals forces, are significant [6].

Mechanical strengths for individual SWNT's have been predicted to be up to 100x that of steel. Experimental values from tensile load testing of SWNT's and MWNT's reported tensile strengths in the range of 11 to 63 GPa [19]. The tensile load does not lead to shell-type instabilities so it is transferred more directly to the chemical bond network. The tensile strength of CNT's may exceed that of many known fibers because of the inherent strength of the carbon-carbon bond [19].

Further interest in CNT's comes from the unique property of CNT's for their high flexibility. Full reversal of bending up to -110^{o} critical angle was observed by Iijima et al [20] without any permanent deformation. The only effects were a stretching of the outer side of the tube and a compression of the inner side. The tube retains its graphitic structure up to very large bending angles showing substantial promise for structural and fiber applications[19].

Dynamic Mechanical Analysis (DMA) is used to characterize polymeric materials. DMA measures the viscoelastic response of materials where a sinusoidal force is applied to a material and the displacement (strain) is measured. A profile of heating at a specified rate or over time at a given temperature is utilized and the response monitored. Storage modulus (E'), loss modulus (E") and tan δ (E''/E') were collected as a function of temperature. DMA has several clamping configurations that include single/dual cantilever, three point bending, tension/compression and shear sandwich modes. The data can be influenced by test

conditions including heating ramp rate, clamp effects, contact stresses, test frequency and test sample alignment. Therefore, it is important to identify which configuration and profile best suits the defined data set for collection.

The activation energy of the glass transition can be determined by applying Arrhenius behavior [21]. Under the application of an external load the specimen deforms upon increasing temperature. A three point bending configuration may be used to eliminate the influence of clamping the sample. As a sinusoidal stress is applied to the composite sample, the strain lags behind the stress due to the viscoelastic response of the polymer. The interfacial bond of the CNT must be strong enough so as to optimally transfer the load from the matrix to the CNT. It is therefore critical that the CNT's be dispersed homogeneously throughout the matrix. The potential of CNT's as structural reinforcement depends critically on the ability to transfer mechanical load from the polymer matrix to the CNT's. If the interfacial bond is weak or the CNT's agglomerate, they only act as nanostructure holes or matrix flaws and the benefits of the properties of the CNT's are not realized[22]. For MWNT's, the weak interaction between the inner and outer tubes limit the stress transfer from the outer tube to the inner tube[23].

CNT's are covalent bonded materials and would have brittle properties at low temperatures. However, the flexibility of CNT's at room temperature is not due to plastic deformation but comes as a result of their high strength and ability of the hexagonal network to distort. The distortion allows for relaxation of the stress [17]. Iijima [20] and Salvetat [17] experimentally observed the bending behavior of CNT's. The formation of pentagonal or heptagonal rings in strained CNT's was observed. The glide line depends on the tube helicity[17]. Studies comparing arc grown and catalytic CNT's found arc grown CNT's to have better properties [24].

In experiments with CNT's in a polymeric film under large compressive strains, buckling was observed [19]. The relaxation of the strain energy caused immediate graphitic to diamond-like bond reconstruction at the site of the collapse [19]. The CNT's when subject to large deformation switch into different shapes. This flexibility comes from the ability of the sp2 C-C bonds to reversibly change hybridization when deformed out of plane [19].

1.6 Applications of Composites

A growing demand for composites with increased mechanical strength, thermal capacity and electrical conductivity arises from potential applications for CNT's. The use of CNT's is of significant interest in aerospace, semiconductor and electronic industries. Many nanocomposite concepts are in the development stage.

To optimize composite material properties using MWNT's, several problems must be overcome. First, the CNT's must be bonded to the surrounding matrix in an efficient way to allow load transfer from the matrix to the tubes. For MWNT's, experiments indicate that only the outer shell supports stress when the MWNT's are dispersed in an epoxy matrix [22]. Second, CNT's have a tendency to agglomerate which must be overcome to achieve uniform dispersion.

Functionalization, with polymeric side groups, of the CNT's is a recent improvement to assist in dispersion and bonding of the nanotubes in a variety of matrices. Chemical treatment of nanotubes adds chemical species on the surface of the tube to facilitate the bonding between tubes and the matrix [24].

2. Experimental Procedure

2.1 Preparation of MWNT Composite

MWNT's having an outer diameter of 5-9 nanometers and average length of 5 microns manufactured by Southwest Nanotechnologies were dispersed in an EPON 828 epoxy resin system. The EPON 828 resin system is a simple bisphenol-A /epichlorhydrin consisting of a short linear chain with epoxide rings at each end. EPON 828 resin (391g) and NADIC Methylanhydride (59g) were weighed to a total of 450 grams. The different mass fractions of MWNT's were dispersed in the resin prior to the addition of the catalyst. Each MWNT sample was dispersed using a Sonic Vibracel 500 watt ultrasonic at 30% power for 45 minutes with a pulse of 10 seconds on and 5 seconds off. To prevent excessive temperature rise during sonication the samples were placed in a cool water bath. Subsequent to sonication, the catalyst N, N Dimethylbenzylamide was added and the samples were baked at 177^{o}C for up to 10 hours and cooled at room temperature. Upon removal and cooling, the samples were cut to size using a Buehler Isomet saw using a 15HC diamond wafering blade. The different mass fractions of MWNTs in all the samples are given in Table I.

Table I – Epoxy-MWNT composite sample identification and mass fraction loading. The mass of resin used in all samples was 450 grams.

Sample	Mass of MWNT (gm)	Mass Fraction of MWNT
A	0.20	0.00044
B	0.50	0.0011
C	1.0	0.0022
D	3.0	0.00667
E	0.1	0.00022
F	0.050	0.00011
Reference	0.0	0.0

One of the difficulties in the use of MWNT's in the composite is to achieve uniform dispersion of the nanotubes in the matrix. An alternate method was also attempted to disperse the MWNT's in the resin using a high shear method. In this method, a Greerco Model 1L homogenizer, as shown in figure 3,was placed in the EPON 828 resin with the MWNT's. The MWNT's were still agglomerated after 1 hour stirring and each cluster was visible and not well dispersed in the resin although the clusters were smaller.

Figure 3: Greerco homogenizer – High shear laboratory scale mixer used to disperse MWNT in epoxy matrix.

2.2 Microscopy

Optical and transmission electron microscopy was carried out to determine the distribution and agglomeration characteristics of the MWNT composite. Optical micrographs were

obtained by placing the sample in the viewing area of a Keyence Model VHX optical microscope with direct lighting. Optical micrographs of several regions in the samples were captured using a digital camera.

The samples were also examined in the Hitachi XF2000 transmission electron microscope. The samples were prepared by FIB (Focused Ion Beam) to thin down a region to electron beam transparency which is about 100nm thickness. The FIB uses a beam of Ga ions to essentially remove material by means of momentum transfer. The heavy Ga ions collide with the sample and atoms from the sample are sputtered off. In this way a thin window is produced for transparency under the TEM.

2.3 Raman spectroscopy

Raman spectroscopy of the sample F was carried out using a Horiba Jobin Yvon MicroRaman spectrometer with a 633 nm HeNe laser. The sample was placed on an aluminum background stage of the Raman spectrometer. A scan of the epoxy with MWNT's dispersed was obtained from Sample F. Separate scans were obtained of pure epoxy for the background and the MWNTs used in the dispersion.

2.4 Dynamic Mechanical Analysis

DMA testing was carried out using a Perkin Elmer DMA 7e with controller TAC 7/DX and connecting chiller Flexi-Cool. The samples for performing these tests had dimensions of 1.5 x 3.5 x 19 mm. Each sample was cut from the prepared MWNT composite using a Buehler Isomet saw. The final dimensions were achieved by light grinding on a Struers Roto-Pol-35. The samples were tested in three-point bending, as shown in figure 4.

The experimental conditions consisted of a heating rate at 15^{o}C/min from 25^{o} to 90^{o}C, at 2^{o}C/min from 90^{o} to120^{o}C, isothermal at 120^{o}C for 3 minutes, and heating rate at 0.1^{o}C/min

from 120^{o} to 170^{o}C. The frequency of the applied sinusoidal load for each experiment was fixed during the entire heating profile (i.e. 1, 2, 3, 5, 10 or 20 Hz). A static force of 110 mN with a displacement of 180 μm was maintained during the experiment in a 3 point bending configuration.

Figure 4. Perkin Elmer DMA 7e, 3 point bending equipment with epoxy composite sample loaded for testing.

2.5 Electrical Resistivity Measurements

Electrical resistance measurements were carried out with a system consisting of a Keithley 236 source meter, Keithley 6514 and 6517 Nanovoltmeters. A K-20 Temperature Control system and a low temperature chamber both from MMR Technologies Inc illustrated in figure 5a were used to vary the temperature of the sample. The temperature was controlled to within +/- 0.1^{o}C. The temperature range was between 250^{o} and 350^{o}C. The source meter was used to supply the minimum current of 1 nanoamp. The given current with the measured

voltage was used to determine the resistance using Ohm's Law, V=IR where V is the voltage, I is the current and R is the resistance.

Figure 5(a). Temperature controlled Dewar and stage used for electrical resistivity measurements of the composite samples.

Electrical resistance measurements were made using a four probe co-linear configuration of contacts, as shown in Figure 5b. Four small dots of colloidal silver paste were applied along the length of the rectangular sample. Gold wires of 0.025 mm diameter and approximately 2 cm long were attached to the silver dots. The free ends of the gold wires were attached for the proper electrical connection. The outer leads were used to input the current from the source meter with the inner leads used to measure voltage across the nanovoltmeter. The reverse current method was used to cancel the thermal electromotive force at the contacts by sending current in the forward and reverse directions. The average value of the two voltage measurements is taken to measure the resistance and resistivity.

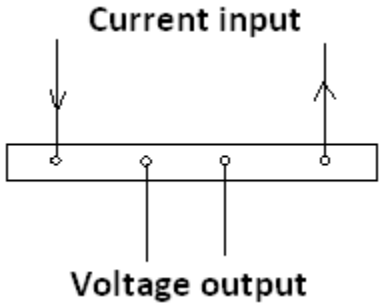

Figure 5(b): Schematic illustration showing the four probe co-linear configuration used for the resistivity measurements.

3. Results

3.1 Microscopy

The MWNT's were observed to be dispersed uniformly containing local regions of agglomeration as seen in the optical micrograph, shown in Figure 6a. Transmission electron micrographs obtained from the sample, shown in figure 6b, showed individual MWNTs with smaller diameter and coalesced MWNTs with larger diameter.

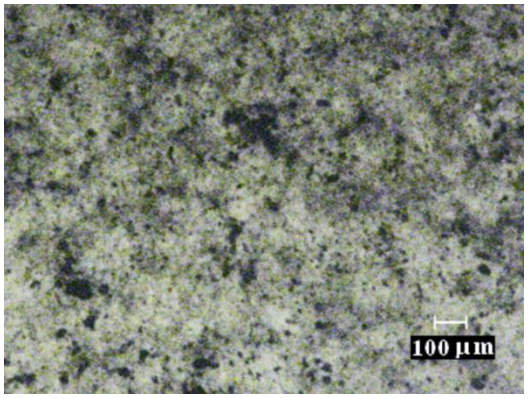

Figure 6(a). Optical micrograph of MWNT epoxy composite showing dispersion of the MWNTs in the epoxy matrix. Agglomeration of the MWNT's is also observed in the form of darker regions.

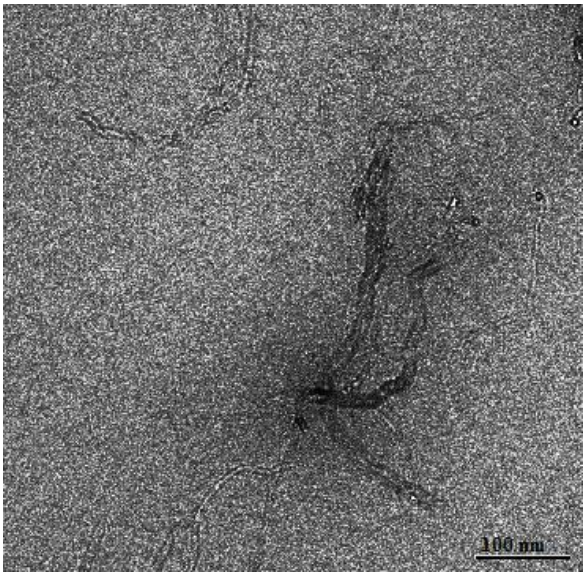

Figure 6(b). TEM image showing MWNT is resin matrix (scale 100 nm). Single MWNT's and agglomerated MWNT's showing dark contrast are observed in the image.

3.2 Raman

Raman spectra for the MWNTs, epoxy and the composite are shown in Figure 7. The Raman spectrum of the composite was found to be a superposition of that of the epoxy and the MWNTs. The results illustrate the presence of the D and G peak in the MWNT with the enhancement of the intensity at the D and 2D peak in the composite shown by the arrows indicating the presence of MWNTs.

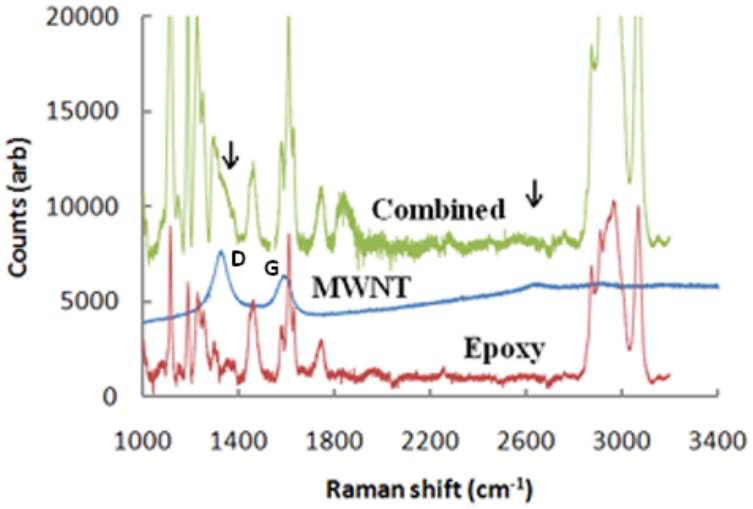

Figure 7. Raman spectra of the bare epoxy, pure MWNT, and composite sample. The D and G peaks are clearly seen. The enhancement of the intensity at the position of the D and the 2D peak shown by the arrows indicates the presence of MWNT.

3.3 DMA Measurements

DMA measurements were carried out at several frequencies (f) for samples A, B and the reference sample to determine the storage modulus (E'), loss modulus (E"), E''/E' or tan (δ)

and the glass transition temperature (T_g). The variation of tan (δ) as a function of temperature (T) was determined at each frequency (f) in the three samples to determine the effect of the MWNT's in the viscous behavior of the composite.

An increase in the test frequency (f) was found to shift the peak of the tan δ to a higher temperature (Tg), in sample B as shown in figure 8a. The variation of tan δ with temperature at f=1 Hz is shown in figure 8b for samples A, B and the reference sample.. The variation of ln(f) with 1/Tg is shown in figures 8c to 8e for samples A, B and reference sample, respectively. A linear variation of ln(f) with 1/Tg with negative slope was observed in all the samples. A larger negative slope was observed in the sample with higher mass fraction of MWNTs. The observed values of Tg at different frequencies in the three samples are shown in Table II.

Table II. Test Frequency (f) and Tg for Samples A, B and Reference Sample.

Sample	Frequency (f)	Tg (^{o}K)
A	1 Hz	406.8
	2 Hz	410.4
	3 Hz	411.4
	5 Hz	415.7
B	1 Hz	402.3
	5 Hz	408.5
	8 Hz	409.4
	20 Hz	413.0
Reference	1 Hz	406.1
	5 Hz	415.6
	10 Hz	420.1

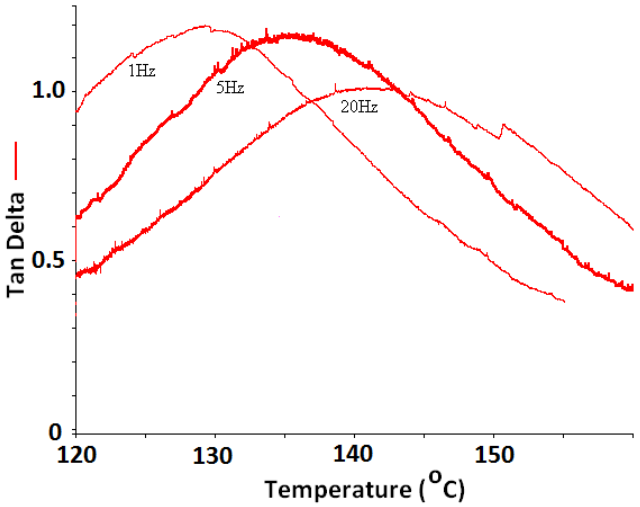

Figure 8(a). Tan δ shown as a function of temperature in sample B for different values of frequency.

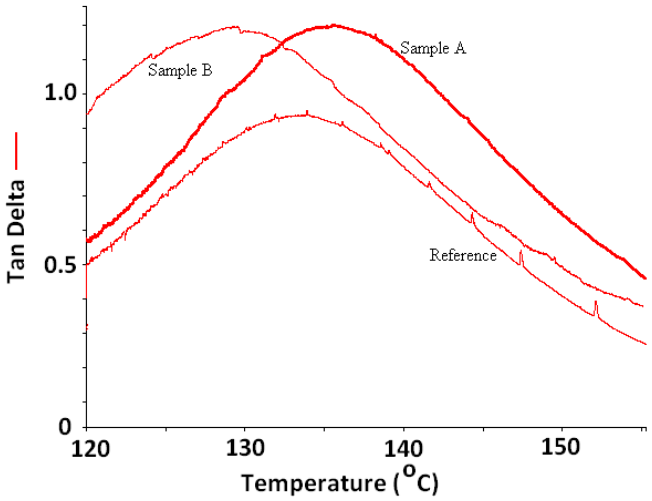

Figure 8(b). Tan δ shown as a function of temperature in samples A, B and reference sample at frequency of 1 Hz.

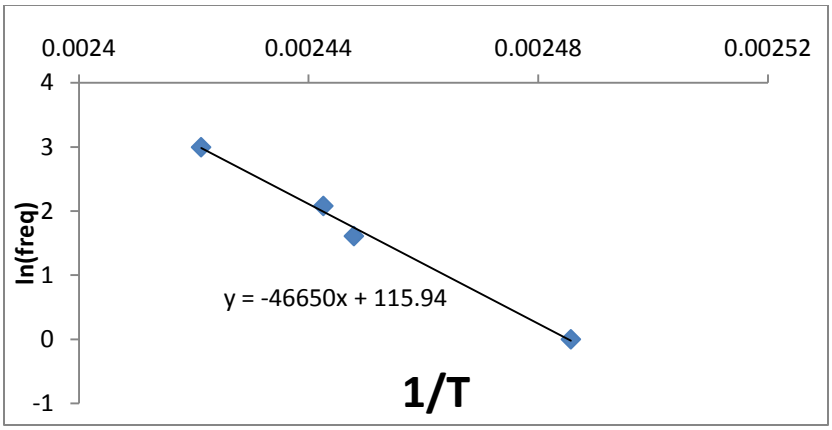

Figure 8(c). Variation of Tg measured from tan δ peak for sample B shown as a function of 1/T. The slope of the curve is directly proportional to the activation energy of the glass transition.

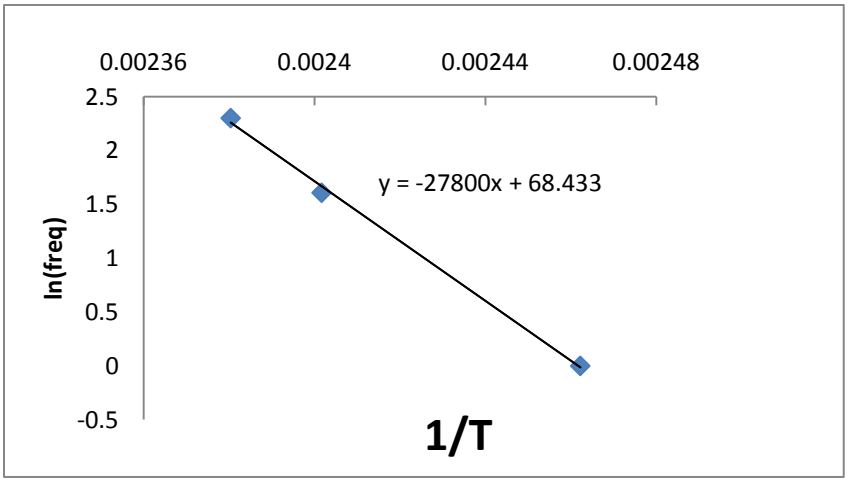

Figure 8(d). Variation of Tg measured from tan δ peak for reference sample shown as a function of 1/T. The slope of the curve is directly proportional to the activation energy of the glass transition.

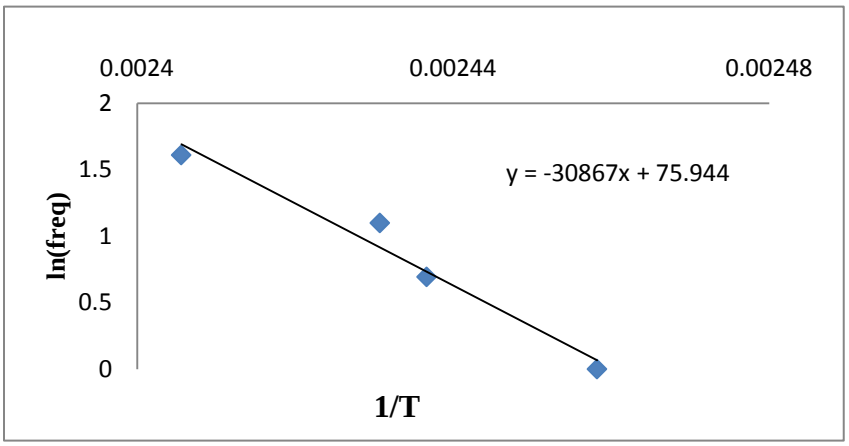

Figure 8(e). Variation of Tg measured from tan δ peak for sample A shown as a function of 1/T. The slope of the curve is directly proportional to the activation energy of the glass transition.

3.4 Electrical Resistivity Measurements

The samples exhibited ohmic behavior in the electrical resistance measurements, as seen in Figure 9a.

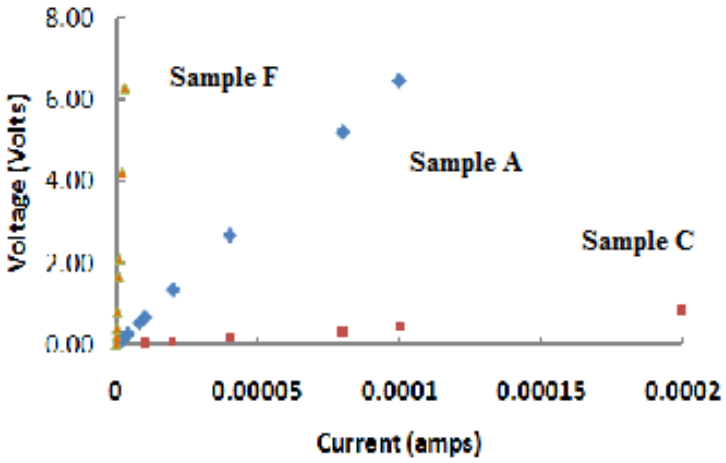

Figure 9(a). Voltage shown as a function of current in the resistivity measurements of the composite samples. The ohmic behavior was observed in samples C, A, and F. These represent low, median and high mass fractions of MWNTs in the samples, respectively.

The resistivity was calculated from the measured voltage (V), current (I), and the thickness (h) of the samples following the equation

$$\sigma = \pi Vh/ [I \ln(2)] \quad (1)$$

The conductivity (ln σ) is shown as a function of mass fraction of MWNT's in Fig. 9b. The predicted variation from percolation behavior of conductivity (ln σ) is shown against mass fraction, m in the inset in figure 9b. Percolation behavior was observed with the rapid increase in conductivity (σ) with a small increase in the weight fraction of MWNTs. The results were found to follow,

$$\sigma = k(m - m_c)^t \quad (2)$$

In the above equation that describes the percolation behavior, t is the exponent that describes the percolation behavior, k is a constant and m_c is the critical mass fraction of MWNTs. The experimental values of ln (σ) are shown fitted to equation (2) in the inset in figure 9b. The value of the critical exponent t was determined to be 1.193 and ln k found to be -0.5577 as shown in the inset plot in Fig. 9b.

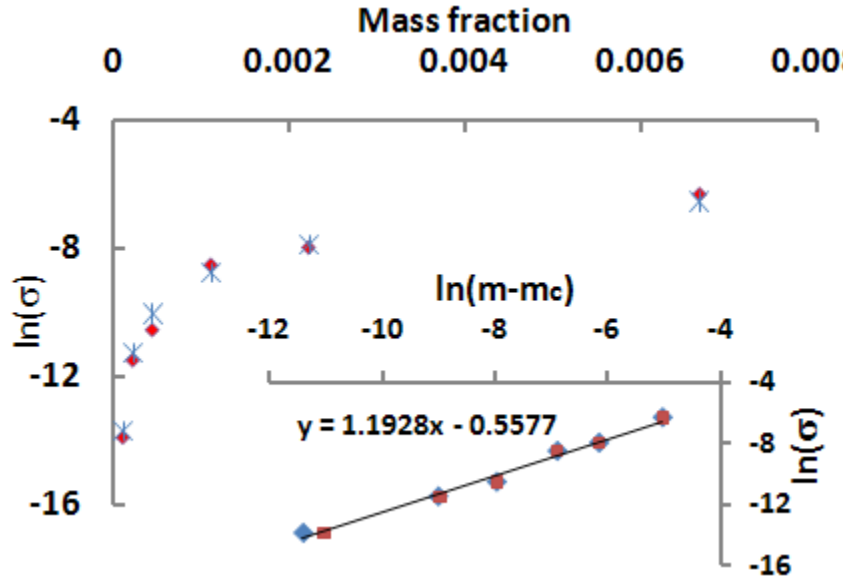

Figure 9(b). The ln(σ) vs mass fraction m shown along with the curve fitted data. The asterisk symbols represent the experimental data and the square symbols represent the curve fitted data. The value of ln(σ) as a function of ln(m-m_c) is shown in the inset. Red squares are for m_c = 0.000095, blue diamonds are for m_c = 0.0001.

The experimental and curve fitted data in figure 9b show good agreement. The temperature dependence of conductivity ln(σ) is shown as a function of 1/T in figure 9c. The slope of ln(σ) versus 1/T was found to be negative and the activation energy was found to be 548.5 J/molK.

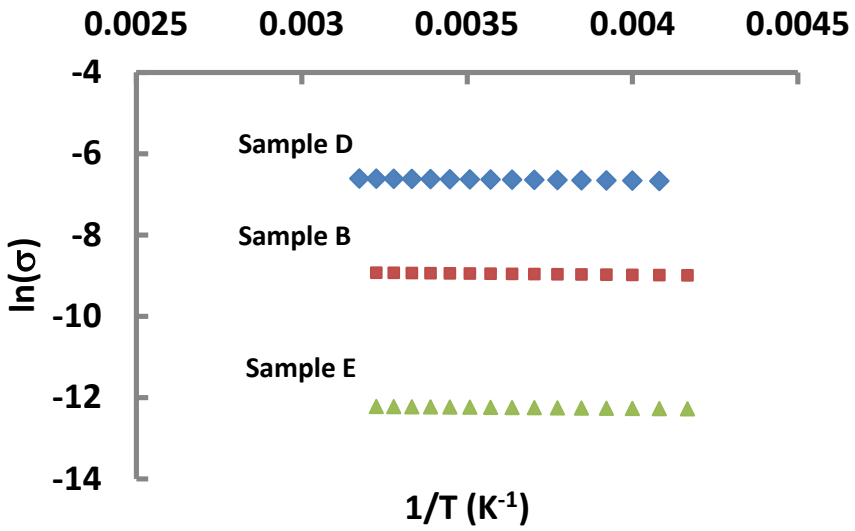

Figure 9(c). The variation of ln(σ) shown as a function of 1/T. A linear behavior was observed for all samples representing low (sample E) to high (sample D) mass fraction of MWNTs.

The temperature dependence of conductivity ln (σ) is also shown as a function of $1/T^{0.25}$ in figure 9d. The slope of ln (σ) versus $1/T^{0.25}$ was also found to be negative and small.

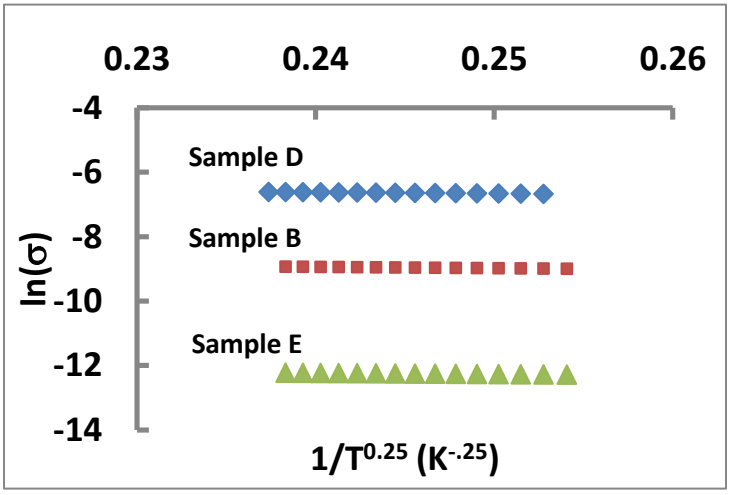

Figure 9(d). The variation of ln(σ) shown as a function of $1/T^{1/4.}$ A linear behavior was observed for all samples representing low (sample E) to high (sample D) mass fraction of MWNT's.

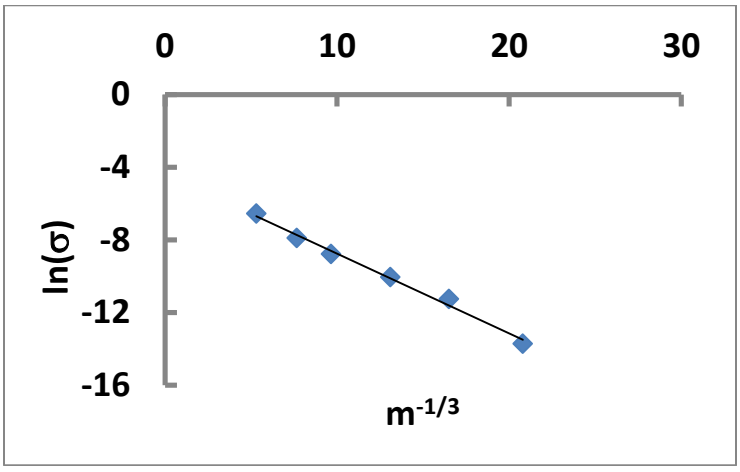

Figure 9(e). Conductivity ln (σ) shown as a function of mass fraction ($m^{-1/3}$) in the composite samples.

4. Discussion

4.1 Optical and Transmission Electron Microscopy

The results of optical microscopy shown in figure 6a illustrate that while there is uniform dispersion of the MWNTs, there are regions wherein MWNTs are agglomerated. The distribution of MWNTs obtained from transmission electron microscopy shown in figure 6b illustrate that individual MWNTs are present separately in addition to coalesced or joined MWNTs. Therefore, the dispersion of the MWNTs is only partially uniform with presence of agglomerated regions.

4.2 Raman Spectroscopy

Raman spectra obtained from MWNTs showed the characteristic D, 2D, G and 2G peaks. These peaks superimposed on the Raman spectrum of the epoxy were found to give rise to an increase in the intensity at the D peak and 2D peak shown by the arrows. Therefore, the Raman spectra are indicative of the composite formation with interfacial continuity.

4.3 Dynamic Mechanical Aanalysis

A shift in the Tg is related to the polymer molecular chain movement as the material is heated through the transition from glassy to rubbery state [25]. The shift allows determination of the activation energy [21] for thermally activated motion of the molecular chains. The effect of temperature on the frequency of conformational changes such as Tg (relaxation) follows

$$f = f_o \exp(-\Delta H/RT) \qquad (4)$$

where f is frequency, f_o is pre-exponential factor, R is universal gas constant, T is Temperature (Kelvin) and ΔH is activation energy associated with molecular motion leading

to viscous behavior. From equation 4, Tg at two different frequencies f_1 and f_2 were used to express the shift in Tg from Tg_1 to Tg_2 in the form,

$$\ln (f_{1/} f_2) = (\Delta H/R) (1/ Tg_2 - 1/ Tg_1) \quad (5)$$

Therefore, the slope of ln(f) versus 1/Tg is equal to - ΔH /R. The activation energy ΔH was calculated from the slope of ln(f) vs. 1/Tg. [21] The results of evaluation of activation energy are shown in Table III.

Table III. Calculated Activation Energy for samples A, B and reference.

Sample	Mass Fraction of MWNT	Calculated Activation Energy ΔH, eV/kJ/mol
Reference	0.0	2.39 / 231.02
Sample A	0.00044	2.84 /256.51
Sample B	0.0011	4.02 / 387.67

The activation energy showed an increase with increase in mass fraction of MWNT's as seen in Table III. These results indicate that MWNTs interact with polymer molecules and restrict the movement through interfacial interaction. The exact nature of the interaction is not clear from these investigations.

The values of Tg, presented in Table II, did not show a systematic variation with the mass fraction of the MWNTs. It is thought that this result is associated with the variation in the structure of epoxy matrix. The final cross linked molecular structure of the epoxy matrix upon curing and addition of the catalyst and the MWNTs was not consistent in all the samples because the ultrasonication was carried out for different time periods to improve the mixing of the MWNTs. These variations could result in different cross-linked molecular

structure locally in the samples and different values of Tg of the matrix. The regions with poor dispersion are thought to give rise to weak regions with lower Tg. However, the activation energy for molecular motion showed an increase with increase in mass fraction of the MWNTs that is consistent with the interaction of the MWNTs with the polymer molecules.

4.4 Electrical Conductivity

Introduction of the MWNTs in the epoxy matrix significantly increased the conductivity of the composite by more than four orders of magnitude. Sample D with $m=6.6x10^{-3}$ showed conductivity of $1.8x10^{-3}$ $ohm^{-1}cm^{-1}$ while sample F with the lowest $m=1.1x10^{-4}$ showed conductivity of $9x10^{-7}$ $ohm^{-1}cm^{-1}$ compared to the insulating epoxy matrix. The temperature range between 250 and 350 K was chosen as the epoxy became brittle at lower temperatures leading to potential cracking that causes a breakdown in electrical conductivity measurement. Also, the sample size was large enough that the temperature could not easily be brought to values lower than 250 K.

Percolation behavior followed power law scaling given by equation (2) as shown in figure 9b. The threshold mass fraction m_c indicates that a physical pathway is formed in the composite such that current flows and a large increase in conductivity is observed for a small increase in m. The average aspect ratio of MWNTs in the composite is close to 1500. The percolation threshold m_c was found to remain close to 0.000095. This value is much smaller than previously observed values in polymer composites. The percolation threshold was reported to be 0.04 for the arc prepared SWNTs in polythiolphene [(11)], 0.0001 for MWNTs in epoxy [(28)], 0.00017 to 0.00028 for MWNTs in epoxy [(29)], 0.0011 for MWNTs in polysulfone [(30)], 0.00012 for MWNTs in epoxy [(31)] and 0.00023 for mixed grade CNTs in epoxy [(32)].

These results indicate that the threshold value is much smaller for epoxy matrix because it is highly insulating. In addition, the threshold mass fraction of CNTs was found to vary and depend on the aspect ratio, processing conditions and purity of MWNTs. Higher threshold value arises from damaged surface, presence of impurities and poor contact between MWNTs [33]. The MWNTs used in the present work are found to be high purity as indicated by the Raman spectrum showing only the peaks associated with MWNTs. The dispersion of the MWNTs is uniform with some agglomeration as illustrated in the optical micrograph shown in figure 6a. The threshold value is smaller for agglomerated CNTs [30] because contact between CNTs is improved.

The value of the critical exponent t=1.193 in equation (2) is smaller and close to 1.3. The parameter t indicates the rate of increase of conductivity close to the threshold. A smaller value of t is responsible for rapid increment in conductivity. The physical interpretation of t is that it is associated with system dimensionality, with a value close to 1.3 for two-dimensional and 2 for three-dimensional networks [26]. A higher value of 2 for SWNTs in polythiolphene [11], 1.44 for MWNTs in epoxy [33], 1.7 to 2 for MWNTs in epoxy [29,31], 1.77 to 2.6 for MWNTs in epoxy [28] and a lower value of 1.02 for CNTs in epoxy [32] were reported. The higher values of t are associated with composites prepared by a process that used shear forces like three-roll milling [31] or calendaring [28].

The value of σ_o in equation (2) is theoretically the intrinsic conductivity of MWNTs. However, the surface condition, poor contact and the electrical contact resistance prevent σ_o from reaching the theoretical value. The observed values are in general much smaller compared to the conductivity of CNTs that is close to 1.85×10^3 $ohm^{-1}cm^{-1}$. The value σ_o from figure 9b is 0.57 $ohm^{-1}cm^{-1}$. This value is higher than 7×10^{-4} [33], 6.7×10^{-4} [34] and

$0.2x10^{-3}$ [29] in MWNT composites reported earlier. The higher value in the present work indicates good electrical contact that is associated with higher purity of surfaces and formation of agglomerates that increased the number of contacts. Further higher values of σ_o equal to 10^3 [31] and $2.3x10^4$ [28] were reported for MWNTs in epoxy that have undergone three-roll milling and calendaring [28]. However, t is much larger in these cases and thus the rate of improvement upon increasing m is not high.

The above results of percolation behavior of MWNT-epoxy composites with low values of threshold m_c and the exponent t and higher σ_o illustrate that the method of processing of the composites using sonication is very efficient. These results may also indicate that the purity of the MWNTs is sufficiently high. It has also been shown [30] that partial agglomeration of the MWNTs at the microscale, as seen in figure 6a, improves the conductivity and reduces the threshold by improving the contact between MWNTs.

Mechanisms of conduction

The linear ln (σ) vs. $1/T^{0.25}$ variation shown in figure 9d in the three samples that covered a wide range of mass fraction of MWNTs indicates variable range hopping (VRH) is applicable. VRH mechanism is characteristic of bundles and mats of CNTs [11] and it is also observed in disordered systems and amorphous semiconductors [35,36]. However, the present observation implies that the hopping of carriers within the agglomerates of MWNTs is the dominant process.

The variation of ln (σ) shown against 1/T in figure 9c is also linear which implies that thermally activated tunneling is followed in the composites. The general expression for thermally activated tunneling in polymer composites is [27,37].

$$\sigma=\sigma_o \exp\{-T_1/(T+T_o)\} \quad (5)$$

which is termed fluctuation induced tunneling (FIT). In the above equation, T_1 is the energy required for an electron to cross the insulator gap between conductive clusters and T_o is the temperature above which the thermally activated conduction over the barrier begins to occur. In the FIT model, composites systems exhibiting conducting behavior are characterized by large conducting regions separated by insulating barriers, such as the epoxy. The conductivity is explained by quantum tunneling. The barrier height decreases with increasing temperature. The values of T_o are usually below 20 K and below 5 K in many MWNT-polymer systems [11] indicating that tunneling is active at slightly higher temperatures. When the temperatures of measurements are higher or $T>>T_o$, the above equation simplifies to thermally activated tunneling given by [11] ,

$$\sigma=\sigma_o \exp(-T_1/T)=\sigma_o \exp(-Q/kT) \quad (6)$$

In the present measurements carried between 250 and 350 K, equation (6) is applicable because $T>>T_o$. The value of activation energy Q is found to be close to 0.0055 eV with negligible variation between different samples. This value of activation energy is quite small compared to thermal energy, kT at higher temperatures used in the present measurements. The applicability of FIT model to the MWNT-epoxy composites in the present work is further checked by the linear relation between ln (σ) and $m^{-1/3}$ shown in figure 9e. It has been shown [26,11,27] that ln (σ) is proportional to the width of the barrier (w) between the conducting regions and w is proportional to $m^{-1/3}$. Therefore, the mechanism of conductivity in the MWNT-epoxy composites in the present work clearly follows the FIT model.

The above results wherein both VRH and FIT models are followed in the higher temperature region of measurements could be a special situation wherein the system behaves like a disordered region with small finely dispersed conducting regions of MWNTs separated

by thin epoxy films. However, the linear dependence of ln (σ) on the width of the barrier is a good indication that the FIT model is applicable.

5. Conclusions

MWNT-epoxy composite samples were prepared using ultrasonication to disperse the MWNT in the epoxy matrix. The composite was cured in an oven at 177^{o}C for 10 hours and cooled at room temperature. The resulting epoxy composites were characterized by optical microscopy and TEM. Electrical resistivity and DMA measurements were performed. The following conclusions were reached:

Composites of epoxy and MWNT can be readily prepared using ultrasonication. The dispersion of the MWNT with this technique shows some agglomerations and uniform distribution of the MWNT's.

Optical microscopy and TEM do not provide a quantitative method of evaluating the level of dispersion of the MWNT's. These may used as a qualitative tool to inspect the variation in the composite.

DMA measurements show an increase in activation energy with an increase in mass fraction of MWNT's. This result indicates stronger interaction between MWNTs and the polymer matrix. However, the value of Tg did not show a systematic increase with the higher mass fraction of MWNT's. Variation of the dispersion levels of the MWNT's throughout the epoxy composite could result in the different Tg values.

MWNT-epoxy composites prepared by sonication showed a four orders of magnitude improvement in electrical conductivity with increase in mass fraction of MWNTs from $1.1x10^{-4}$ to $6.6x10^{-3}$. The percolation behavior of electrical conductivity is found to follow with very small value of threshold mass fraction of MWNTs, critical exponent and higher

value of conductivity associated with MWNTs. The higher purity of MWNTs, uniform dispersion and agglomeration of MWNTs with good contact are considered responsible for the improved conductivity.

The temperature dependence of the electrical conductivity in the range of 250 to 350 K is found to follow the VRH and FIT models. However, the linear dependence of conductivity on the width of the epoxy barrier separating the MWNTs is taken as a more clear evidence that FIT model is followed. The results of the present work suggest that use of high purity MWNTs with sonication to disperse in the epoxy polymer is a simple procedure to process high electrical conductivity composites.

The strength of the epoxy composites depends on the ability to transfer the mechanical load to the CNT's. The activation energy for viscous deformation increased with higher mass fraction of MWNTs indicating MWNT -matrix interaction to be present.

6. Future Scope

Experimental procedure to synthesize the composites has to be improved to reduce the variation in the epoxy cross linking and maintain uniform MWNT dispersion in the composite. All samples should also be tested using Differential Scanning Calorimetry (DSC) to evaluate degree of cure and variation from sample to sample.

REFERENCES

1. Iijima, S., *Nature*, **354** 56, (1991).

2. Dresselhaus, M. and Endo, M., Relation to Other Carbon Materials, Ch 2, p 14 in Carbon Nanotubes, edited by Dresselhauss, M., Dresselhaus, G., Avouris, Ph., Springer Technology & Eng.,2001, Berlin.

3. http://en.wikipedia.org/wiki/Carbon_nanotube

4. Khare, R. and Bose, S., *J. of Minerals & Materials Characterization and Eng* , **4** (2005).

5. Forro, L., Schonenberger, C., Physical Properties of MWNT, Ch 13, p 392 in Carbon Nanotubes, edited by Dresselhaus, M., Dresselhaus, G., Avouris, Ph., Springer Technology & Eng.,2001, Berlin.

6. Wilson, M., Nanotechnology:Basic Science and Emerging Technologies, CRC Press (2002).

7. Wilson, M., *AZoNanotechnology* Article, (2006).

8. Qin, L. C. , *J of Materials Science Letters*, 457-459, (1997).

9. Toubestani, H.D. and Ghoranneviss, M., et al, *Macrol Symp*, **287** 143-147, (2010).

10. Wilson, M., Nanotechnology:Basic Science and Emerging Technologies, (2002).

11. Kymakis, E. and Amaratunga, G. A. J , *J. of Applied Physics*, **99** (2006).

12. Hong, S. and Min, S., *Nature Nanotechnology*, 2 (4) 2007

13. Tans, S.J., Devoret, H., Thess, A., Smalley, R.E., Gerligs, I.J. and Dekker,C., *Nature*, **386** 474, (1997).

14. Liang, G.D. and Tjong S. C, *Materials Chemistry and Physics*, **100** 132 (2006).

15. Kyrylyuk, A. V. et al, *Nature Nanotechnology*, (2011).

16. Liu, L. et al, *Physica E* **24** 343 2004

17. Salvetat, J.P., Bonard, J.M., Thomson, N.H., Kulik, A.J., Forro, L., Benoit, W. and Zuppirroli, L., *Appl Phys*, **69**, 255-260, (1999).

18. Yakobson, B. and Avouris, Ph., Mechanical Properties of CNT, Ch. 12, p 322 in Carbon Nanotubes, edited by Dresselhauss,M., Dresselhaus, G., Avouris, Ph., Springer Technology & Eng.,2001, Berlin.

19. Salvetat, J.P., and Rubio, A., *Carbon*, **40** 1729-1734, (2002).

20. Iijima, S., Brabec, C., Maiti,A. and Bernholc,J., *J. Chem. Phys.* **104** 2089-2092, (1996).

21. Li, G., Sullivan,P.L. and Thring, P. R.W., *J. Thermal Analysis & Calorimetry*, **60** 377-390 (2000).

22. Pantano, A., Modica, G., and Cappello, *J. Materials Sci & Eng*. **486** 222-227 (2008).

23. Goh, H.W., Goh,S.H., Xu, G.Q., Pramoda, K.P. and Zhang,W.D., *Chemical Physics Letters* **373** 277-283 (2003).

24. Harris, P.J.F., *International Materials Reviews* **49** 31-43 (2004).

25. Bao, S.P. and Tjong, S.C., *Materials Sci. & Eng*. **485** 508-516 (2008).

26. Bauhofer, W. and Kovacs, J. Z., *Compo. Sci. Techn*., **69**, 1486(2009).

27. Connor, M. T., Roy, S., Ezquerra, T. A., Balta ,Calleja F. *J. Phys*. Rev. B, 57, 2286(1998).

28. Kovacs, J. Z., Mandjarov, R. E., Blisnjuk, T; Prehn, K., Sussiek, M., Muller J., Schulte K;., and Bauhofer, W., *Nanotechnology*, 20, 1(2009).

29. Kim, Y. J; Shin, T. S., Choi, H. D., Hwon, J. H., Chung, Y-C. and Yoon H. G, *Carbon*, 43, 23(2005).

30. Aguilar, J. O; Bautista Quijano J. R. and Aviles, F., *eXpress Polymer Lett*., 4, 292(2010).

31. Rosca, I. D., and Hoa, S. V., *Carbon*, 47, 1958.

32. Thakre, P. R., Bisrat, Y. and Lagoudas, D. C., *J. Appl. Poly. Sci*., 116, 191 (2010).

33. Barrau, S., Demont, P., Peigney, A., Laurent C. and Lacabanne, C, *Macromolecules*, 36, 5187(2003).

34. Ouanies, Z., Park, C., Wise, K. E., Sicohi, E. J. and Harrison J. S., *J. Compos. Sci. Techn*., **63** 1637-46 2003,

35. Mott, N. F. and Davis, E.A; Electronic Properties in Non-Crystalline Materials, Oxford, Clarendon, 1971.

36. Ambegaokar, V., Halperin, B. I. and Langer, J., *J. Non-Crystalline Solids* **8-10** 492-496 1972

37. Sheng, P., *Phys. Rev*. B; 21, 2180 (1980).